Compositional Kernels to Facilitate Multi-Fidelity Design Analysis: Applications for Early-Stage Design

Nikoleta Dimitra Charisi
Mekelweg 2
2628 CD Delft
NETHERLANDS

N.D.Charisi@tudelft.nl

Austin Kana
Mekelweg 2
2628 CD Delft
NETHERLANDS

A.A.Kana@tudelft.nl

Hans Hopman
Mekelweg 2
2628 CD Delft
NETHERLANDS

J.J.Hopman@tudelft.nl

Keywords: Multi-fidelity models; Gaussian processes; compositional kernels; uncertainty quantification; early-stage design.

ABSTRACT

For effective early-stage decision making, engineers need to explore the design space via assessing a large number of possible solutions. Traditionally, for ship design, early-stage exploration is based on low fidelity analysis. However, for novel designs, high fidelity analysis is required early on in the design process for the assessment of the different solutions. Low fidelity tools are not able to capture the complex physics often associated with the performance of novel designs. For such cases, multi-fidelity models have been proven beneficial. The paper investigates how compositional kernel search applied to a framework based on the linear autoregressive scheme (AR1) of multi-fidelity Gaussian Processes can facilitate the analysis of complex engineering systems, such as naval vessels. The method has been applied to benchmark functions, including the Forrester and the ND Rosenbrock functions, and also to a simplified design problem of a cantilevered beam. The results show improved predictions in terms of higher accuracy and reduced uncertainty compared to using less high fidelity analysis data. The method shows promise in introducing high fidelity analysis earlier on in the design process, and in addressing challenging early-stage design applications.

1.0 INTRODUCTION

Early-stage design of complex systems, such as naval vessels, is considered by many to be one of the most critical design phases because that is when many of the major design decisions are made, and as a consequence, most of the costs (approximately 70% of the total lifecycle cost according to Dierolf and Richter, 1989) are committed. One of the major challenges is that engineers need to make these big decisions

with limited knowledge of the design, since knowledge is gradually gained throughout the process (Mavris *et al.,* 1998). Knowledge regarding the performance of the design is important to making informed design decisions (Seyffert, 2018) and in turn, better designs. To assess the performance of each design, knowledge is generated via analysis methods and tools. Traditionally, the fidelity of these tools gradually increases throughout the design process (Figure 1). Early-stage design exploration is based on low fidelity (LF) tools such as simplified physical models, data from reference designs, empirical and semi-empirical methods. LF tools are suitable for a broad exploration of the design space but lack in accuracy. Conversely, high fidelity (HF) tools such as experiments and computationally expensive numerical simulations are used later on the process when the design space is limited to few promising solutions. HF tools can capture accurately the underlying physics of the problem and thus, these tools offer accurate predictions.

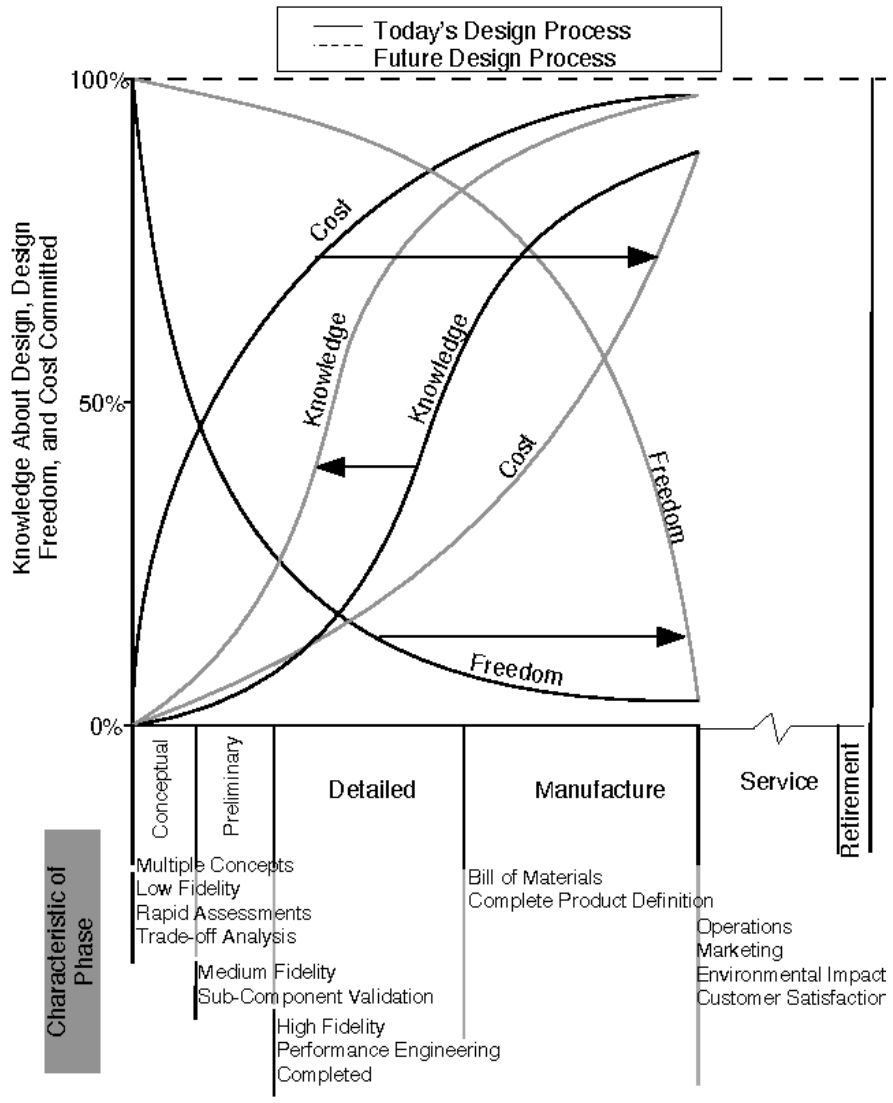

Figure 1: The stages of the design process (Mavris et al.1998).

However, there are cases that this approach is not sufficient. For example, the hydro-structural assessment of a tumblehome ship hull requires using HF tools (e.g., Kim, Park and Kim, 2022), whereas LF tools are sufficient for traditional hull forms (e.g., Nikolopoulos and Boulougouris, 2019). Typically, these cases connect with designs incorporating novel features such as the tumblehome hull of the US Navy DDG1000 frigate designed to improve stealth by minimizing the cross radar section. LF tools are not effective for these cases due to the

complex physics that needs to be captured. On the other hand, HF tools are able to capture the physics of complex problems but are computationally expensive. As a consequence, designers can only assess a limited number of designs with HF tools. However, for effective early-stage decision making, designers need to explore the design space requiring a large number of designs to be assessed. This is a challenge which can be addressed by introducing multi-fidelity (MF) models in early-stage design applications.

MF models are a current state-of-the-art for early-stage design in various engineering fields such as aerospace (e.g., Di Fiore et al., 2021), automotive (e.g., Bertram, Othmer and Zimmermann, 2018) and ship design (e.g., Bonfiglio, Perdikaris, Vernengo *et al*., 2018). There are different definitions for MFMs in literature. According to Beran *et al*. (2020),

> *analysis or design of a system is considered MF when there is synergistic use of different mathematical descriptions (i.e., different physics typically represented by different governing equations, boundary conditions, or parametric attributions) in the analysis or design procedure.*

The HF model ensures that the relevant physics is taken into account, whereas the LF models achieve computational speed-ups.

There are three main ways to combine models for building MF models, known as model management strategies (Peherstorfer, Willcox and Gunzburger, 2018): adaptation, fusion, and filtering. Various MF schemes have been proposed for different methods using these model management strategies. For example, MF models based on Gaussian Processes (GPs) (e.g., Bonfiglio, Perdikaris, Vernengo *et al*., 2018), Monte Carlo (MC) (e.g., Ng and Willcox, 2014), and Artificial Neural Networks (ANNs) (e.g., Zhang *et al.*, 2021) are widely applied for design analysis and optimization problems. GPs are strong and well-understood mathematical methods that provide robust predictions including the underlying uncertainty associated with the predictions. Uncertainty quantification is important for decision-making problems (Bickel and Bratvold, 2008), such as early-stage design. For vehicle design applications requiring computationally expensive analysis, GPs offer a great advantage since they provide good predictions based on limited training data. Linear (see Kennedy and O'Hagan, 2000) and nonlinear (see Damianou and Lawrence, 2012; Perdikaris *et al*, 2017) MF schemes have been proposed for the GPs. For vehicle design, the linear scheme has been successfully applied to different problems such as the shape optimization of super-cavitating hydrofoils (Bonfiglio, Perdikaris, Brizzolara, and Karniadakis 2018). The present paper focuses on the linear scheme autoregressive model (AR1) proposed by (Kennedy and O'Hagan, 2000).

For design applications, one the main challenges is that a larger HF dataset is required to achieve accurate predictions for more complex and higher dimensional problems. Building a larger HF dataset is a challenge because each data point is the outcome of computationally expensive analysis or even experiments. Thus, there is limited (computational) budget available for the acquisition of the HF dataset. To address this challenge the authors propose the application of compositional kernels, originally proposed by Duvenaud *et al*., (2013), to achieve more accurate predictions with less HF data. To the best of the authors knowledge, compositional kernels have not been applied to MF schemes. Focusing on the two-level multi-fidelity case, we propose a two-stage approach to build compositional kernels for the MF-GP framework. The first stage is to build a compositional kernel for the LF model based solely on the LF analysis data, and the second stage is to build a compositional kernel for the HF model based on the MF analysis data. The main idea of the proposed method is to facilitate design analysis and optimization via the discovery of the underlying structure of the HF model. In this way, more accurate predictions can be achieved by using less HF data and thus, the required computational cost can be reduced. The proposed method is applied to benchmark functions and to a simplified design problem.

The paper organizes as follows. Section 2.0 provides a detailed description of the proposed method. Section 3.0 illustrates the case studies and shows the results. Section 4.0 discusses the conclusions.

2.0 METHODS

2.1 Proposed Method

The proposed method has two main building blocks: the compositional kernels and the multi-fidelity GPs. Figure 2 shows the way these building blocks are combined. In this section, a detailed description of the proposed method and its main building blocks is given.

The authors propose the application of compositional kernels to improve the predictions of the linear autoregressive scheme (AR1) scheme. The approach consists of two-steps; the first step is to build a compositional kernel for the $k_{\mathrm{L}}(x, x'; \theta_{\mathrm{L}})$ based on a single fidelity GP model (mathematical formulation in Section 2.2.1) for the low fidelity data, and the second step is to build a compositional kernel for the $k_{\mathrm{H}}(x, x'; \theta_{\mathrm{H}})$ based on the MF GP model (mathematical formulation in Section 2.2.2) using both the low and the high fidelity data. Searching the structure of the compositional kernels is a discrete optimization problem. Compositional kernels consisting of a small number of basis kernels can be constructed via discrete exhaustive search. Conversely, compositional kernels consisting of a large number of basis kernels require the use of optimization algorithms for discrete problems such as genetic algorithms. The layers of the compositional kernel, or the number of basis kernels, is determined by the complexity of the underlying structure of the physical problem. The Bayesian Information Criterion (BIC) [Equation (16)] was used as the search criterion.

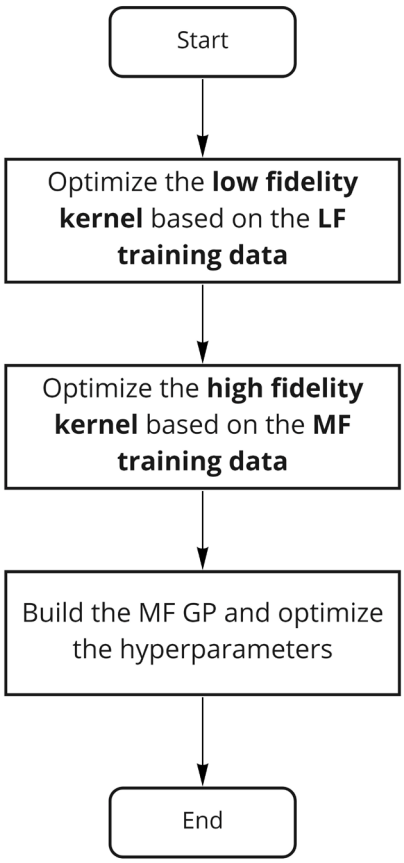

Figure 2: Flowchart of the proposed method.

2.2 Multi-Fidelity Gaussian Processes

2.2.1 Gaussian Processes

The Gaussian process (GP) regression is used to build approximations of real world processes. A Gaussian process is 'a collection of random variables, any finite number of which have a joint Gaussian distribution, and it is fully characterized by its mean and covariance function' (Rasmussen and Williams, 2006). The GP of a real world process *f(x)* is fully defined by its mean *m(x)* and covariance *k(x,x')* function as follows (Rasmussen and Williams, 2006):

$$m(x) = \mathbb{E}[f(x)] \tag{1}$$

$$k(x,x') = \mathbb{E}\big[\big(f(x) - m(x)\big)\big(f(x') - m(x')\big)\big] \tag{2}$$

Therefore,

$$f(x) \sim \mathcal{GP}\big(m(x), k(x,x';\theta)\big) \tag{3}$$

For engineering problems, the available analysis or experimental data are considered as noisy observations of the underlying function. The available data have the following form:

$$y = f(x) + \epsilon,\ \epsilon \sim \mathcal{N}(0, \sigma_n^2 I) \tag{4}$$

where y represents our observations, f is the function to be approximated, and ϵ is the error term. The prior distribution of the observed data X and the test data X_* is the following:

$$\begin{bmatrix} y \\ f_* \end{bmatrix} \sim \mathcal{N}\left(\begin{bmatrix} 0 \\ 0 \end{bmatrix}, \begin{bmatrix} K(X,X) + \sigma_n^2 I & \mathrm{K}(\mathrm{X},\mathrm{X}_*) \\ \mathrm{K}(\mathrm{X}_*,\mathrm{X}) & \mathrm{K}(\mathrm{X}_*,\mathrm{X}_*) \end{bmatrix}\right) \tag{5}$$

where f_* the function values evaluated at X_*. The GP belongs to the family of Bayesian methods. For Bayesian methods, a critical element of the analysis is the prior which encodes our prior knowledge or assumptions regarding the unknown function *f*. A common practice is to assign the prior a zero mean and a kernel function $k(x,x';\theta)$ where θ is a vector of hyperparameters. Based on the kernel function, the covariance matrix is constructed as follows: $K_{ij} = k(x_i, x_j; \theta)$. According to Bayesian learning, the prior distribution is updated by taking into account the observed data. More specifically, the prior distribution is conditioned on the observed data to get the posterior distribution

$$f_* | X, X_*, y \sim \mathcal{N}(\mu_*, \sigma_*^2) \tag{6}$$

$$\mu_* = k_*^{\mathrm{T}}[K + \sigma_n^2 I]^{-1} y \tag{7}$$

$$\sigma_*^2 = k_{**} - k_*^{\mathrm{T}}[K + \sigma_n^2 I]^{-1} k_* \tag{8}$$

where $K = K(X,X)$, $k_{**} = k(x_*, x_*)$, and $k_* = k(x_*)$.A commonly applied method to optimize the hyperparameters of the kernel function is to maximize the marginal log-likelihood defined as:

$$\log p(y|x,\theta) = -\frac{1}{2}\log|K + \sigma_n^2 I| - \frac{1}{2} y^T (K + \sigma_n^2 I)^{-1} y - \frac{n}{2}\log 2\pi \tag{9}$$

2.2.2 Multi-Fidelity Gaussian Processes

In this section, the AR1 scheme for multi-fidelity GPs (MF-GPs) proposed by Kennedy & O'Hagan (2000)is shown. The method assumes that there is a linear dependency between the different fidelities. More specifically, the high- and low-fidelity functions are associated as follows:

$$f_t(x) = \rho_{t-1} f_{t-1}(x) + \delta_t(x) \tag{10}$$

where the t=1,…,s is the increasing fidelity level, f_{t-1} and f_t are GPs, ρ is a scaling parameter, and $\delta_t \sim \mathcal{GP}\left(\mu_{\delta_t}, k_t(x_t, x_t'; \theta_t)\right)$ is an additive term. The method assumes that:

$$\mathrm{cov}\{f_t(x), f_{t-1}(x') | f_{t-1}(x)\} = 0, \forall x \neq x'. \tag{11}$$

The aforementioned property ensures that we cannot learn more about $f_t(x)$ from any other $f_{t-1}(x')$ given $f_{t-1}(x)$. For the two-level multi-fidelity problem, we have observations

$$y_H = f_H(x) + \epsilon_H, \epsilon_H \sim \mathcal{N}\left(0, \sigma_{n_H}^2 I\right). \tag{12}$$

$$y_L = f_L(x) + \epsilon_L, \epsilon_H \sim \mathcal{N}\left(0, \sigma_{n_L}^2 I\right). \tag{13}$$

The underlying functions are associated via Equation (10) as follows

$$f_H(x) = \rho_L f_L(x) + \delta_H(x) \tag{14}$$

In addition, $f_L \sim \mathcal{GP}\left(0, k_L(x, x'; \theta_L)\right)$ and $\delta_H(x) \sim \mathcal{GP}\left(0, k_H(x, x'; \theta_H)\right)$ are considered two independent GPs. It is a common assumption to consider GPs with a zero mean prior, which does not restrict the posterior mean to be zero (Rasmussen and Williams, 2006). Based on the autoregressive assumption, the low and high fidelity observations are jointly distributed as follows:

$$\begin{bmatrix} y_L \\ y_H \end{bmatrix} \sim \mathcal{N}\left(\begin{bmatrix} 0 \\ 0 \end{bmatrix}, \begin{bmatrix} k_L(x_L, x_L'; \theta_L) + \sigma_{n_L} I & \rho k_L(x_L, x_H'; \theta_L) \\ \rho k_L(x_H, x_L'; \theta_L) & \rho^2 k_L(x_H, x_H'; \theta_H) + k_H(x_H, x_H'; \theta_H) + \sigma_{n_H} I \end{bmatrix}\right) \tag{15}$$

The covariance matrix of Equation (15) is used to calculate the posterior distribution [Equations (6)-(8)]. For the training of the model, the hyperparameters are optimized based on the maximization of the marginal log likelihood [Equation (9)].

2.3 Compositional Kernels

The most critical element of the GP is the covariance matrix, or the kernel, because it encodes our prior assumptions regarding the prediction. The requirements for a kernel to be valid is to be: (1) symmetric and (2) positive semidefinite. Previous research has developed basis functions which can be used to build valid covariance matrices. The kernel expresses the similarity between the data points (Rasmussen and Williams, 2006). For example, the periodic kernel capture successfully functions which repeat themselves exactly. Duvenaud *et al.*, (2013) developed compositional kernels defined as kernels constructed by adding or multiplying a small number of basis kernels. The idea of the method was to decompose the function to be learned into interpretable components. The composition of the kernels is based on a search method aiming to minimize the Bayesian information criterion (BIC) metric defined as:

$$BIC = k\ \ln(n) - 2\ln(L) \tag{16}$$

where n is the number of training data, k are the number of hyperparameters, and L is the maximized likelihood value. One of the main components of BIC is the likelihood function. In addition, it introduces a penalty term based on the model's parameters to avoid complexity and overfitting.

3.0 RESULTS

In this section, the results of three case studies are presented, including: the assessment of the benchmark Forrester and ND Rosenbrock functions, and the structural assessment of a simplified cantilever beam problem. The case studies of the analytical functions have L1 (quantities of interest (QoIs) are analytical functions, negligible computational cost) level of complexity and the case study of the cantilever beam has L2 (QoIs are computed via solving ODEs or PDEs, moderate computational cost) level of complexity as defined by AVT-331 (Beran *et al*. 2020). For the shown case studies, the python packages, Emukit (Paleyes et al., 2021) and GPy (GPy, 2012), were used.

3.1 Forrester Function (1D)

The Forrester function is a one-dimensional test function proposed by Forrester, Sbester and Keane (2007). This function has been proposed as a benchmark function for MF optimization methods by Mainini *et al.*, (2022) and has been widely applied to demonstrate frameworks based on MF-GPs (i.e., Kontogiannis and Savill, 2020). The two-fidelity function is described by Equations (17) and (18):

$$f_{\mathrm{H}}(x) = (6x-2)^2 \sin(12x-4), x\epsilon[0,1] \tag{17}$$

$$f_{\mathrm{L}}(x) = 0.5 f_{\mathrm{H}}(x) + 10(x-0.5) - 5, x\epsilon[0,1] \tag{18}$$

The Forester function is used to visualize the idea of how compositional kernels can improve the predictions of the MF model. In this case we used 5 HF and 25 LF training points. In Figure 3, the prediction of the function by using the reference and the proposed model can be seen. The reference model implements the AR1 scheme of the MF-GPs, as described in Section 2.2.2, with the squared exponential (SE) kernel. The SE kernel is widely applied in relevant literature (e.g., Bonfiglio, Perdikaris, Vernengo *et al.*, 2018). By capturing the structure of the underlying function [Figure 3(c) and Figure 3(d)] via using compositional kernels, the model is able to make more accurate predictions. In this case, the optimization of the compositional kernels' structure was extended up to combining two basis kernels. The SE kernel was used as k_{L}. For the k_{H}, the linear kernel was multiplied by the matern 3/2. For further information on the mathematical formulation of the different kernels, the reader is referred to (Rasmussen and Williams, 2006).

3.2 ND Rosenbrock Function (ND)

The second case is the ND Rosenbrock function, which has been proposed as a benchmark function for higher dimensional MF optimization problems by Mainini *et al.*, (2022). The two-fidelity function is described by the Equations (19) and (20), and visualized in Figure 4:

$$f_{\mathrm{H}}(x) = \sum_{i=1}^{D-1} 100(x_{i+1} - x_i^2)^2 + (1-x_i)^2, x\epsilon[-2,2] \tag{19}$$

$$f_{\mathrm{L}}(x) = \frac{f_{\mathrm{H}}(x) - 4 - \sum_{i=1}^{D} 0.5x_i}{10 + \sum_{i=1}^{D} 0.25x_i}, x\epsilon[-2,2] \tag{20}$$

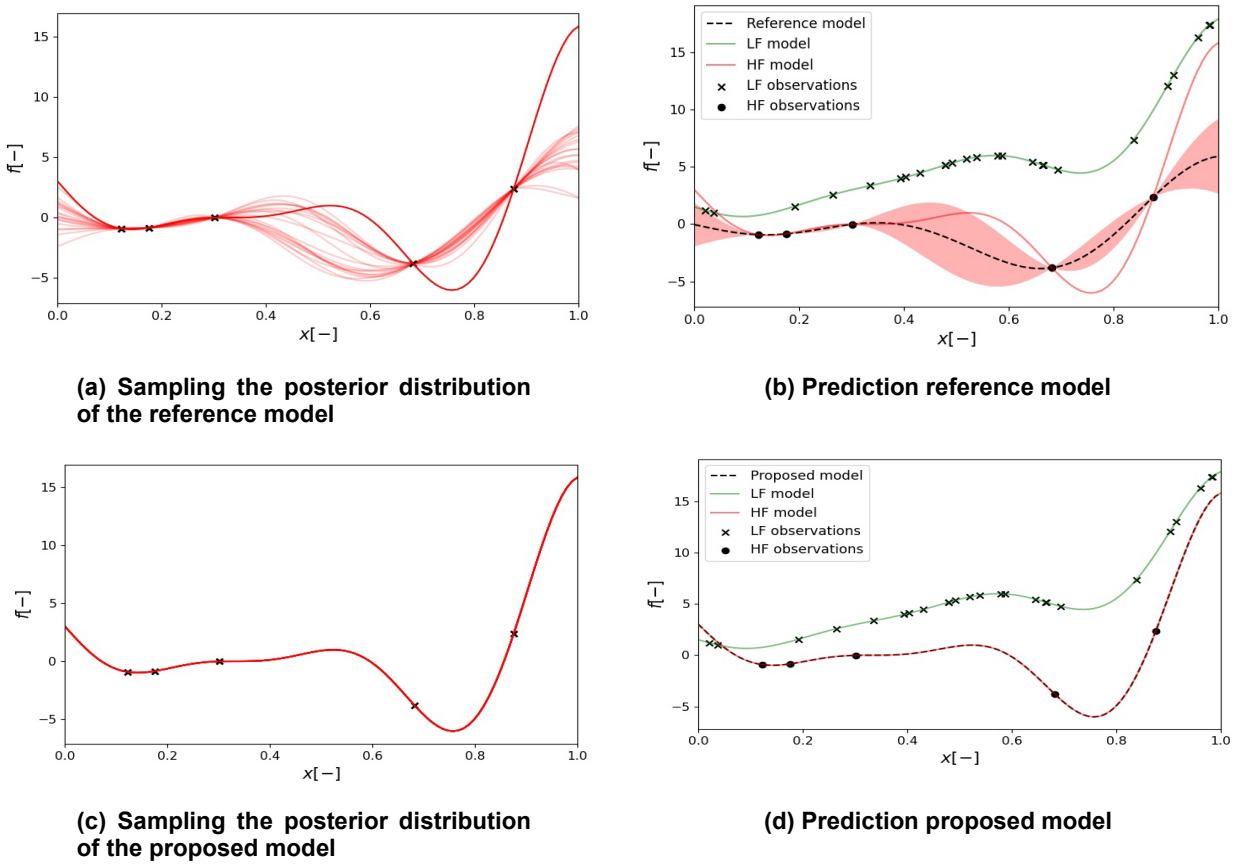

(a) Sampling the posterior distribution of the reference model

(b) Prediction reference model

(c) Sampling the posterior distribution of the proposed model

(d) Prediction proposed model

Figure 3: Sampling the posterior distribution for the Forester function.

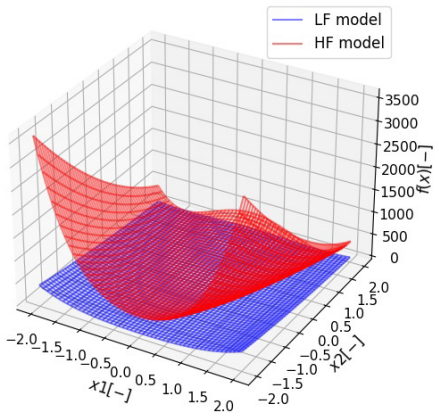

Figure 4: 2D Rosenbrock function.

Design optimization problems are multi-dimensional. This function offers the opportunity to better simulate the design problem since its dimensionality can be increase. To assess the performance and robustness of the proposed method, two case studies were performed. The first investigates the accuracy of the method's predictions while changing the number of the HF training points. The second case study investigates the

accuracy of the method's predictions while increasing the dimensionality of the function. Both case studies closely relate to the challenge that a larger HF dataset is required to achieve accurate predictions for more complex and higher dimensional design problems.

3.2.1 Study on Increasing the Number of the HF Data

For this case study, we assumed that N=2, used 70 LF points, and increased the number of HF points from 10 to 50. The sampling method was Latin Hypercube Sampling (LHS). The analysis was performed on 17 different training sets. Two different metrics, the coefficient of determination R^2 and the normalized root mean squared error (RMSE), were computed to assess the quality of the prediction. The results of the different models are compared by calculating the improvement based on the normalized RMSE. The results are summarised in Table 1, and the calculated improvement is shown in Table 2. In addition Figure 5(a)-Figure 5(b) show how the predictions fit the HF function in two cross sections ($x1 = 1.1431, x2 = 1.1431$) of the domain. The results showed significant improvement for limited HF data.

Table 1: Results 2D Rosenbrock function.

DoE	GP HF R^2	GP HF RMSE	Reference model R^2	Reference model RMSE	Proposed model R^2	Proposed model RMSE
	mean (std)	mean (std)	mean (std)	mean (std)	mean (std)	mean (std)
(10,70)	-3.0203E-02 (2.2350E-01)	2.2815E-01 (2.7447E-01)	4.1191E-01 (8.3273E-01)	9.8460E-02 (8.3860E-02)	9.9367E-01 (4.9214E-03)	1.2885E-02 (3.7570E-03)
(20,70)	2.5570E-01 (4.3959E-01)	1.8084E-01 (7.3824E-02)	9.4046E-01 (1.3028E-01)	2.7634E-02 (3.0494E-02)	9.9550E-01 (4.2670E-03)	1.0276E-02 (4.7369E-03)
(30,70)	7.6553E-01 (3.7365E-01)	7.3497E-02 (8.1344E-02)	9.7203E-01 (4.2800E-02)	2.2934E-02 (1.6418E-02)	9.9265E-01 (9.7394E-03)	1.2330E-02 (7.5569E-03)
(40,70)	9.4037E-01 (2.3021E-01)	2.2625E-02 (5.0445E-02)	9.9359E-01 (5.4596E-03)	1.2484E-02 (5.1453E-03)	9.9394E-01 (1.1012E-02)	1.0271E-02 (8.1770E-03)
(50,70)	8.6489E-01 (3.6932E-01)	3.7230E-02 (7.4430E-02)	9.8949E-01 (7.7966E-03)	1.6056E-02 (6.4166E-03)	9.9526E-01 (7.4690E-03)	9.3859E-03 (6.8252E-03)

Table 2: Computed improvement for the 2D Rosenbrock function.

DoE	Improvement ref. model compared to GP HF	Improvement prop. model compared to GP HF	Improvement prop. model compared to the ref. model
(10,70)	56.8%	94.4%	86.9%
(20,70)	84.7%	94.3%	62.8%
(30,70)	68.8%	83.2%	46.2%
(40,70)	44.8%	54.6%	17.7%
(50,70)	56.9%	74.8%	41.5%

3.2.2 Study on Increasing the Dimensions

This case study assesses the proposed method as the problem dimensions increased. The dimensions of the ND Rosenbrock were varied from 2 to 10. For the analysis, we used 50 HF observations and 70 LF observations. The training sets were sampled via LHS. In order to assess the robustness of the method, the analysis was performed on 17 different training sets. The results are shown in Table 3 and Table 4.

Table 3: Results ND Rosenbrock function.

Dimensions	GP HF R^2 mean (std)	GP HF RMSE mean (std)	Reference model R^2 mean (std)	Reference model RMSE mean (std)	Proposed model R^2 mean (std)	Proposed model RMSE mean (std)
2	5.8304E-01 (4.4563E-01)	1.1344E-01 (9.2215E-02)	9.2676E-01 (1.1984E-01)	3.5022E-02 (2.9269E-02)	9.9629E-01 (6.3662E-03)	8.1115E-03 (6.3137E-03)
4	3.3938E-02 (1.1383E-01)	6.6610E-01 (4.4552E-02)	4.2990E-01 (3.3225E-01)	4.9264E-01 (1.4253E-01)	7.6025E-01 (1.1122E-01)	3.2396E-01 (7.5234E-02)
6	6.2616E-03 (3.3051E-02)	1.1283E+00 (1.9389E-02)	3.2985E-01 (2.3779E-01)	9.1182E-01 (1.6550E-01)	6.0034E-01 (1.4977E-01)	7.0232E-01 (1.3746E-01)
8	6.1005E-03 (2.9700E-02)	1.5798E+00 (2.4308E-02)	2.9246E-01 (3.0442E-01)	1.3109E+00 (2.4208E-01)	6.1580E-01 (1.4393E-01)	9.6372E-01 (1.9037E-01)
10	-9.4176E-04 (8.8841E-04)	2.0386E+00 (9.0454E-04)	2.4017E-01 (1.8684E-01)	1.7642E+00 (2.0614E-01)	5.1448E-01 (1.5481E-01)	1.4023E+00 (2.2243E-01)

Table 4: Computed improvement for the ND Rosenbrock function.

Dimensions	Improvement ref. model compared to GP HF	Improvement prop. model compared to GP HF	Improvement prop. model compared to the ref. model
2	69.1%	92.8%	76.8%
4	26.0%	51.4%	34.2%
6	19.2%	37.8%	23.0%
8	17.0%	39.0%	26.5%
10	13.5%	31.2%	20.5%

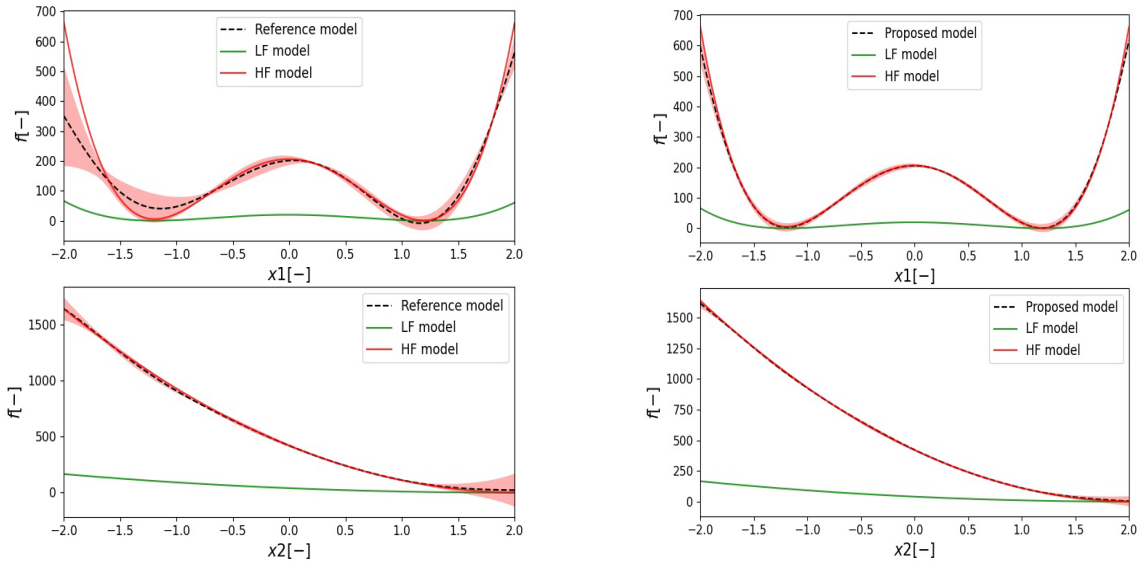

(a) Prediction reference model. **(b) Prediction proposed model.**

Figure 5: Cross section of the predicted posterior distribution at x1=1.1431 and x2=1.1431.

3.2 Simplified Design Problem

As a simplified design problem, a cantilever beam structural problem (Figure 6) was tested. The problem was retrieved from (Brevault, Balesdent and Hebbal, 2020). The problem is a two-fidelity problem, where the LF method is the analytical estimation of the maximal von Mises (VM) stress and the HF method is the numerical estimation of the maximal VM stress.

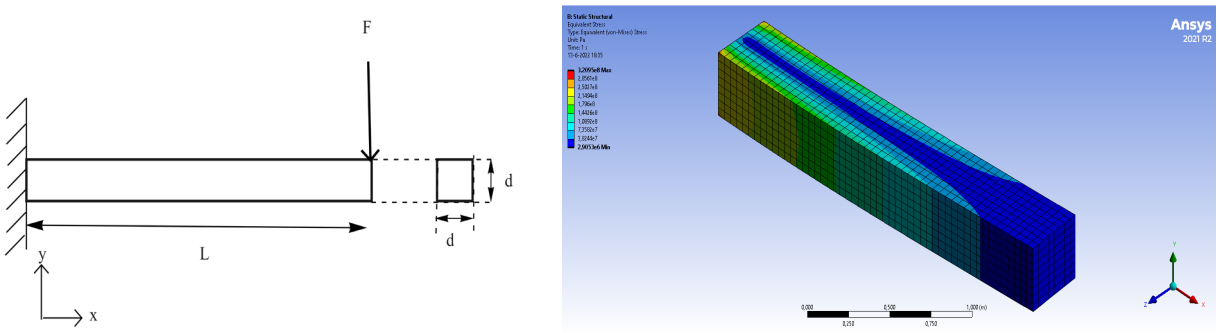

(a) Schematic representation of the cantilever beam problem **(b) Equivalent von Mises stresses calculated by Ansys software**

Figure 6: Cantilever beam structural problem.

Regarding the analytical calculation of the VM stress, the shear force and the bending moment acting along the length of the beam subjected to a transverse force need to be taken into account. The maximal bending stress is calculated by:

$$\sigma_b = -\frac{M_b(\frac{d}{2})}{I} \quad (21$$

$$M_b = -FL \quad (22$$

where M_b: the bending moment, I: moment of inertia ($I = d^4/12$ for square cross sections), F: applied force, and L: beam's length. The average shear force is calculated as follows:

$$\tau = \frac{FQ}{Id} \quad (23$$

where Q: the first moment of area, with respect to the neutral axis, that lies above the point of interest ($Q = d^3/8$), and d: side of the square cross section. The maximal VM stress is calculated by Equation (24).

$$\sigma_{VM}^{max} = \sqrt{\sigma_b^2 + 3\tau^2} \quad (24$$

For the numerical model, a hole was introduced on the basis of the cantilever beam. The dimensions of the hole were defined as a function of the beam's main dimensions ($l_{hole} = 0.3L, d_{hole} = 0.3d$). Steel was defined as the beam's material with the following properties: $E = 2E + 11$ GPa, and $\nu = 0.30$. The structural problem was modelled as a 2D problem with L, d the independent variables. The problem domain was defined by $L\epsilon[2.0,3.0]$ m and $d\epsilon[0.25, 0.4]$ m. The applied force was set to 950.0 kN. The results are summarised in Table 5 and Table 6. The results showed that the reference and the proposed model offer more accurate predictions than the GP based on the HF data (17.3% and 19.9% respectively). However, the accuracy of the three models gets similar to each other when increasing the number of HF data.

Table 5: Results structural problem.

DoE	GP HF R^2 mean (std)	GP HF RMSE mean (std)	Reference model R^2 mean (std)	Reference model RMSE mean (std)	Proposed model R^2 mean (std)	Proposed model RMSE mean (std)
(5,60)	5.6891E-01 (2.7050E-01)	9.7890E-02 (3.5613E-02)	6.9703E-01 (2.1436E-01)	8.0970E-02 (3.2709E-02)	7.1597E-01 (2.1306E-01)	7.8376E-02 (3.1727E-02)
(10,60)	8.1878E-01 (1.1246E-01)	6.3344E-02 (2.3429E-02)	8.2822E-01 (1.1481E-01)	6.1307E-02 (2.3777E-02)	8.3341E-01 (1.1553E-01)	6.0092E-02 (2.4131E-02)
(20,60)	9.5018E-01 (3.4122E-02)	3.3951E-02 (1.0074E-02)	9.5117E-01 (3.7931E-02)	3.3336E-02 (1.0858E-02)	9.5186E-01 (3.8218E-02)	3.3022E-02 (1.1012E-02)

Table 6: Computed improvement for the structural problem.

DoE	Improvement ref. model compared to GP HF	Improvement prop. model compared to GP HF	Improvement prop. model compared to the ref. model
(5,60)	17.3%	19.9%	3.2%
(10,60)	3.2%	5.1%	2.0%
(20,60)	1.8%	2.7%	0.9%

4.0 CONCLUSIONS AND DISCUSSION

4.1 Recommendations for Further Research

The proposed method aims to eventually facilitate design optimization. In the present paper, the case studies show the benefit associated with design analysis. Thus, the next step is to explore the potential of the method applied to design optimization. In addition, a two-level multi-fidelity setup was examined. Therefore, the applicability of compositional kernels to multi-fidelity problems with multiple LF models is a topic for future research. Finally, the method was tested to benchmark functions and a simplified design problem. Consequently, the potential benefit of the method when potential when applied to a realistically complex design problem should be explored.

4.2 Conclusions

Early-stage design of complex systems is challenging due to the lack of knowledge inherent to these systems. This paper proposed the integration of compositional kernels in a MF-GP framework to facilitate design analysis and optimization. We applied the method to analytical benchmark functions and a cantilever beam structural problem. The analytical functions include the Forrester function, and the ND Rosenbrock function. We used the ND Rosenbrock function to test the influence of the number of the HF data and the problem dimensions to the accuracy of the predictions. For the cantilever beam problem, the LF analysis data were derived from solving the analytical equations for the estimation of the maximal VM stress, whereas the HF analysis data was taken by solving a FEM model in Ansys. The results showed that the proposed model performed better than the reference model, especially in limited HF data regimes. In addition, the uncertainty bounds associated with the prediction decreased. The uncertainty reduction leads to more confidence on the model predictions and in turn, facilitates decision making. Although the method was not applied to a complex engineering problem, the overall results showed significant improvement in the prediction and reduction of the uncertainty associated with it. Therefore, the proposed method seems promising for facilitating design analysis to support decision making for early-stage design applications.

ACKNOWLEDGEMENTS

This publication is part of the project “Multi-fidelity Probabilistic Design Framework for Complex Marine Structures” (project number TWM.BL.019.007) of the research programme “Topsector Water & Maritime: the Blue route” which is (partly) financed by the Dutch Research Council (NWO). The authors thank DAMEN, the Netherlands Defence Materiel Organisation (DMO), and MARIN for their contribution to the research.

5.0 REFERENCES

Beran, P., Bryson, D., Thelen, A., Diez, M., and Serani, A. (2020), "Comparison of Multi-Fidelity Approaches for Military Vehicle Design", AIAA AVIATION 2020 FORUM.

Bertram, A., Othmer, C. and Zimmermann, R. (2018), "Towards Real-time Vehicle Aerodynamic Design via Multi-fidelity Data-driven Reduced Order Modeling", in AIAA/ASCE/AHS/ASC Structures, Structural Dynamics, and Materials Conference proceedings in Reston, Virginia, USA, 2018, American Institute of Aeronautics and Astronautics.

Bickel, J.E. and Bratvold, R.B. (2008), "From Uncertainty Quantification to Decision Making in the Oil and Gas Industry", Energy Exploration & Exploitation, Vol. 26 No. 5, pp. 311-325.

Bonfiglio, L., Perdikaris, P., Brizzolara, S. and Karniadakis, G. (2018), "Multi-fidelity optimization of super-cavitating hydrofoils", Computer Methods in Applied Mechanics and Engineering, Vol. 332, pp. 63-85.

Bonfiglio, L., Perdikaris, P., Vernengo, G., de Medeiros, J. and Karniadakis, G. (2018), "Improving SWATH seakeeping performance using multi-fidelity Gaussian process and Bayesian optimization", Journal of Ship Research, Vol. 62 No.4, pp. 223-240.

Brevault, L., Balesdent, M. and Hebbal, A. (2020), "Overview of Gaussian process based multi-fidelity techniques with variable relationship between fidelities, application to aerospace systems", Aerospace Science and Technology, Vol. 107, p. 106339.

Damianou, A., and Lawrence, N.D. (2013), "Deep Gaussian Processes", in Proceedings of the Sixteenth International Conference on Artificial Intelligence and Statistics, Scottsdale, Arizona, USA, 2013, Proceedings of Machine Learning Research, Vol. 31, pp. 207-215.

Di Fiore, F., Maggiore, P. and Mainini, L. (2021), "Multifidelity domain-aware learning for the design of re-entry vehicles", Structural and Multidisciplinary Optimization, Vol. 64 No. 5, pp.3017-3035.

Dierolf, D.A. and Richter, K.J. (1989), "Computer-Aided Group Problem Solving for Unified Life Cycle Engineering (ULCE)", available at: https://apps.dtic.mil/sti/citations/ADA209446

Duvenaud, D., Lloyd, J., Grosse, R., Tenenbaum, J. and Zoubin, G., (2013), "Structure Discovery in Nonparametric Regression through Compositional Kernel Search", in Proceedings of the 30th International Conference on Machine Learning in Atlanta, Georgia, USA, 2013, Proceedings of Machine Learning Research, Vol. 28 No. 3, pp.1166-1174.

GPy. (2012), "GPy – A Gaussian Process (GP) framework in Python", available at: http://github.com/SheffieldML/GPy

Kennedy, M.C. and O'Hagan, A. (2000), "Predicting the Output from a Complex Computer Code When Fast Approximations Are Available", Biometrika, Vol. 87 No. 1, pp. 1-13.

Kim, B.S., Park, D.M. and Kim, Y. (2022), "Study on nonlinear heave and pitch motions of conventional and tumblehome hulls in head seas", Ocean Engineering, Vol. 247, p. 110671.

Kontogiannis, S. and Savill, M. (2020), "A generalized methodology for multidisciplinary design optimization using surrogate modelling and multifidelity analysis". Optimization and Engineering, Vol. 21 No. 3, pp.723-759.

Mainini, L., Serani, A., Rumpfkeil, M.P., Minisci, E., Quagliarella, D., Pehlivan, H., Yildiz, S., Ficini, S., Pellegrini, R., Di Fiore, F., Bryson, D., Nikbay, M., Diez, M., Beran, P. (2022), "Analytical Benchmark Problems for Multifidelity Optimization Methods", in *arXiv*, available at: https://arxiv.org/abs/2204.07867v1

Mavris, D., DeLaurentis, D., Bandte, O. and Hale, M. (1998), "A stochastic approach to multi-disciplinary aircraft analysis and design", in 36th AIAA Aerospace Sciences Meeting and Exhibit proceedings, Reston, Virginia, USA, 1998.

Ng, L. and Willcox, K. (2014), "Multifidelity approaches for optimization under uncertainty", International Journal for Numerical Methods in Engineering, Vol. 100 No. 10, pp.746-772.

Nikolopoulos, L. and Boulougouris, E. (2019), "A Study on the Statistical Calibration of the Holtrop and Mennen Approximate Power Prediction Method for Full Hull Form, Low Froude Number Vessels", Journal of Ship Production and Design, Vol. 35 No. 01, pp. 41-68.

Paleyes, A., Pullin, M., Mahsereci, M., McCollum , C., Lawrence, N.D. and Gonzalez, J. (2021), "Emulation of physical processes with Emukit", in *arXiv*, available at: https://arxiv.org/abs/2110.13293

Peherstorfer, B., Willcox, K. and Gunzburger, M. (2018), "Survey of Multifidelity Methods in Uncertainty Propagation, Inference, and Optimization", SIAM Review, Vol. 60 No. 3, pp.550-591.

Perdikaris, P., Raissi, M., Damianou, A., Lawrence, N. and Karniadakis, G. (2017), "Nonlinear information fusion algorithms for data-efficient multi-fidelity modelling". Proceedings of the Royal Society A: Mathematical, Physical and Engineering Sciences, Vol. 473 No. 2198, p.20160751.

Rasmussen, C.E. and Williams C.K.I. (2003), Gaussian Processes in Machine Learning, Cambridge, MIT Press.

Seyffert, H. . (2018) Extreme Design Events due to Combined, Non-Gaussian Loading. PhD Thesis. The University of Michigan.

Zhang, X., Xie, F., Ji, T., Zhu, Z. and Zheng, Y. (2021), "Multi-fidelity deep neural network surrogate model for aerodynamic shape optimization", Computer Methods in Applied Mechanics and Engineering, Vol. 373, p.113485.